

## Seismic Response of Steel Structures Equipped with the Seesaw System

Panagiota S. Katsimpini<sup>a</sup>, George A. Papagiannopoulos<sup>a</sup>, Dimitris L. Karabalis<sup>\*,a</sup>

<sup>a</sup>University of Patras, Dept. Civil Engineering, Greece  
penyk@hotmail.gr, gpapagia@upatras.gr, karabali@upatras.gr

### ABSTRACT

This work provides seismic response results from non-linear seismic analyses of low-rise 3-D steel structures equipped with the seesaw system. In particular, seismic response results involving height wise distributions for peak interstorey drift ratios (IDR) and peak residual interstorey drift ratios (RIDR) as well as plastic hinge formations are obtained for 2- and 8-storey fixed-base steel structures. Additionally, soil-structure interaction (SSI) is considered for these steel structures and its effect in the aforementioned seismic response results is discussed. It is concluded that the seesaw system constitutes an attractive solution for low-rise 3-D steel structures as buckling problems associated with common steel braces are eliminated.

**Keywords:** seesaw system, steel structures, seismic analysis, soil-structure interaction

### 1 INTRODUCTION

The seesaw system consists of a pin-supported seesaw, two spiral strand ropes (cables) with turnbuckles that intersect from the edges of the seesaw and a couple of dampers installed vertically on the seesaw. Figure 1 displays a simple steel frame equipped with a seesaw system, whereas variations of this system regarding its installation and configuration type as well as the kind of dampers used (fluid viscous, viscoelastic, slit) can be also found in literature.

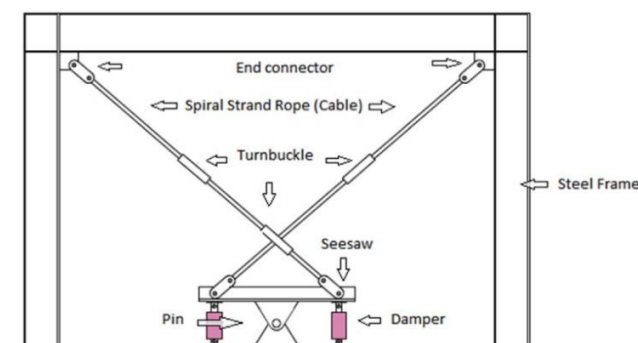


Fig. 1. A steel frame equipped with the seesaw system

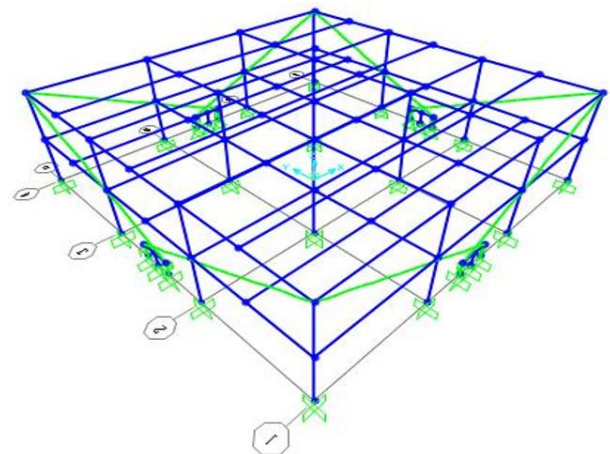


Fig. 2. 2-storey steel structure with seesaw system

From the numerical and experimental investigations performed in (1), it has been concluded that the seesaw system can significantly reduce the seismic response of plane steel frames and increase their damping capacity. The purpose of this paper is to present preliminary seismic response results regarding the application of the seesaw system in low-rise 3-D steel structures. These response results involve height wise distributions for peak interstorey drift ratio (IDR) and peak residual interstorey drift ratio (RIDR) and are obtained firstly by considering the steel structures to be fixed-

base and then by taking into account soil-structure (SSI). Worst cases of plastic hinge formation to the steel structures are also shown for both the fixed-base and SSI cases. It is concluded that the seesaw system, essentially working always in tension, constitutes an attractive bracing solution for low-rise 3-D steel structures

## 2 SEISMIC ANALYSIS OF LOW-RISE 3-D STEEL STRUCTURES

### 2.1 Steel structures with seesaw system

The 2- and 8-storey steel structures studied are shown in Figs.2-3, where the seesaw system (its spiral strand ropes are shown with green colour) is installed at every side of the frames of their perimeter. The spiral strand ropes emanating from the seesaw device are anchored at both ends of the beams of the perimeter and at the same floor level. There is no eccentricity of the seesaw system with the respect to the frame where it is installed. On the other hand, slotted holes are assumed to exist at the flanges of some beams and columns so that the spiral strand ropes can pass through them.

For the steel structures shown in Figs.2-3, each bay has 6.0 m span and each storey has 3.0 m height. Diaphragm action is assumed at every floor due to the presence of a composite slab. Dead and live loads on the composite slabs are considered  $8 \text{ kN/m}^2$  and  $3 \text{ kN/m}^2$ , respectively. The steel structures are initially designed as typical concentrically braced frames according to Eurocodes 3 and 8 (2,3) and the storey shear computed from spectrum analysis is used in order to estimate the diameter of the spiral strand ropes of the seesaw system. The design seismic load is calculated using the design spectrum of Eurocode 8 (3) that corresponds to peak ground acceleration (PGA) of  $0.36 \text{ g}$ , soil class B and behaviour factor equal to 3. Final sections for columns and beams as well as the diameter and the design tensile breaking strength of the spiral strand ropes (4) are tabulated in Tables 1 and 2 for the 2- and 8-storey structures, respectively. The steel grade employed is S235 for beams and S355 for columns and all connections of steel members are considered as moment-resisting ones. Column orientation for both steel structures follows Fig.4.

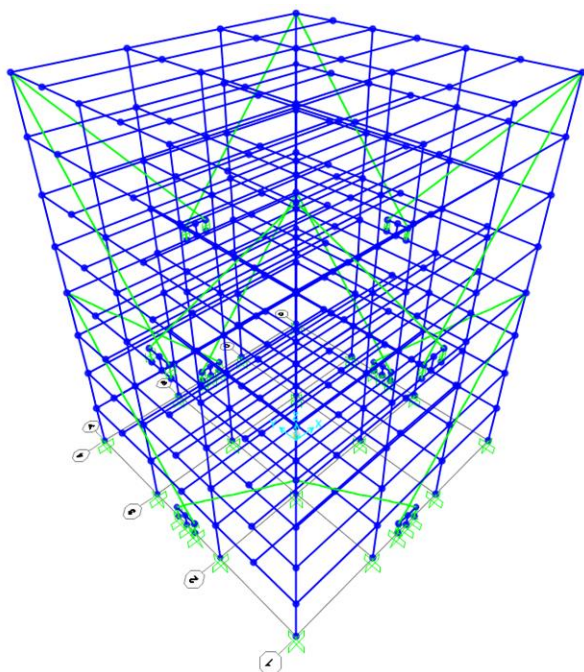


Fig. 3. 8-storey steel structure with seesaw system

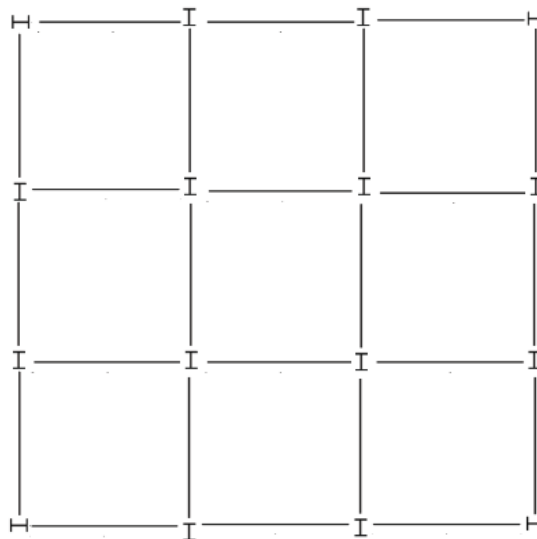


Fig. 4. Orientation of columns for the 2- and 8-storey steel structures

A small initial prestressing is also taken into account for the spiral strand ropes and it is also assumed that their anchorage type is such that the tensile breaking strength values of Tables 1 and 2 do not need to be reduced according to (4). Linear viscous dampers having a damping coefficient of  $250 \text{ kNs/m}$  are employed. Referring to Fig. 1, the maximum height of the vertical steel plates of the

seesaw is limited by the mid-stroke length of the dampers. Thus, the height of the vertical steel plates of the seesaw is 870 mm. Three vertical steel plates are used and essentially form a truly pinned connection (name as ‘pin’ in Fig. 1). The middle plate of this pinned connection is welded to the bottom area of the horizontal steel plate of the seesaw. The length of the horizontal steel plate is 1600 mm.

Table 1. Sections for the 2-storey steel structure

Storeys	Column	Beam	Spiral strand rope (mm) – Tensile breaking strength (kN)
1 – 2	HEM320	IPE450	48 – 1440

Table 2. Sections for the 8-storey steel structure

Storeys	Column	Beam	Spiral strand rope (mm) – Tensile breaking strength (kN)
1 – 8	HEM700	IPE500	115 - 8270

## 2.2 Seismic ground motions, soil-structure interaction and modelling for non-linear seismic analysis

The steel structures of Figs.2-3 are subjected to the two horizontal components of the 24 seismic ground motions presented in Table 3. An angle of seismic incidence equal to 0°, 90° and 180° is also taken into account for these components. Several details about these earthquake ground motions concerning location, date, recording station, moment magnitude  $M_w$  and soil type can also be found in Table 3. Regarding soil type, the abbreviations HR, SR and SL correspond to hard rock, sedimentary and conglomerate rock and soil/alluvium, respectively.

Table 3. Seismic ground motions

No.	Earthquake, Location	Date	Recording Station	$M_w$	Soil Type
1.	San Fernando, U.S.A.	09/02/1971	Pacoima Dam	6.6	HR
2.	Imperial Valley, U.S.A.	15/10/1979	El Centro Array 6	6.5	SL
3.	Valparaiso, Chile	03/03/1985	Llolleo	7.9	SR
4.	Michoachan, Mexico	19/09/1985	SCT	8.0	SL
5.	Vrancea, Romania	30/08/1986	INCERC	7.3	SL
6.	Superstition Hills, U.S.A.	24/11/1987	Parachute Test Site	6.5	SL
7.	Loma Prieta, U.S.A.	17/10/1989	Los Gatos	7.0	HR
8.	Cape Mendocino, U.S.A.	25/04/1992	Cape Mendocino	6.9	SR
9.	Cape Mendocino, U.S.A.	25/04/1992	Petrolia	6.9	SR
10.	Landers, U.S.A.	28/06/1992	Lucerne Valley	7.3	SL
11.	Northridge, U.S.A.	17/01/1994	Rinaldi Receiving St.	6.7	SL
12.	Northridge, U.S.A.	17/01/1994	Newhall	6.7	SL
13.	Northridge, U.S.A.	17/01/1994	Sylmar Converter St.	6.7	SL
14.	Kobe, Japan	17/01/1995	Takatori	6.9	SL
15.	Chi-Chi, Taiwan	20/09/1999	TCU 052	7.6	SL
16.	El Salvador, El Salvador	13/01/2001	Observatorio	7.6	SR
17.	Denali, Alaska	03/11/2002	Taps Pump station 10	7.9	SR
18.	Bam, Iran	26/12/2003	Bam	6.5	SL
19.	Ica Pisca, Peru	15/08/2007	ICA2	8.0	SL
20.	Maule, Chile	27/02/2010	Constitution	8.8	SR
21.	Darfield, New Zealand	03/09/2010	Greendale	7.0	SL
22.	Christchurch, New Zealand	22/02/2011	Lyttelton Port Company	6.3	SL
23.	Christchurch, New Zealand	22/02/2011	Resthaven	6.3	SL
24.	Kefalonia, Lixouri	03/02/2014	Lixouri	6.1	SR

Inclusion of SSI in seismic analyses is performed by employing the discrete model of (6). According to this model the foundation and its surrounding soil are effectively replaced by a spring-dashpot-mass system that takes into account horizontal and vertical translations, rocking and torsion. The values of the spring-dashpot-mass system are calculated on the basis of the dimensions of the foundation using the formulas provided in (6). For the steel structures under study, raft foundations are designed considering a soil class D (3,7). The shear modulus of this soil class (computed using a shear wave velocity of 180m/sec and a soil density of 1900kgr/m<sup>3</sup>) is reduced to 40% of its initial value in order to take into account the exhibition of non-linear soil deformations in soft soils for large levels of ground acceleration (7).

The seismic response of the steel structures of Figs.2-3 is determined through nonlinear analyses using (5). Geometrical non-linearities are also taken into account. Beams and columns are modelled using standard frame elements with concentrated plasticity and 2% strain hardening. Axial-flexural interaction is considered for the plastic hinges of the columns. Diaphragm action is assumed at every floor, whereas the innate viscous damping of the steel structure is considered to be 3%. Linear viscous dampers are modelled as discrete damping elements using the 'Link element' of (5). The horizontal and vertical steel plates of the seesaw are modelled as rigid elements, whereas the spiral strand ropes are modelled as cable elements considering geometrical non-linearities and also a small pretension.

### 3 SEISMIC RESPONSE RESULTS

The seismic response results of this section involve only the unfavourable structural responses taking into account the previously mentioned values of the angle of seismic incidence.

#### 3.1 Fixed-base steel structures

The 2-storey steel structure of Fig. 2 exhibits nonlinear behaviour to 23 out of the 24 seismic ground motions of Table 3. The maximum tensile strength of the spiral strand ropes is exceeded for 2 out of the 24 seismic ground motions of Table 3, whereas no damper failure occurred. Height wise peak IDR and RIDR distributions for the 2-storey steel structure are shown in Figs.5-6.

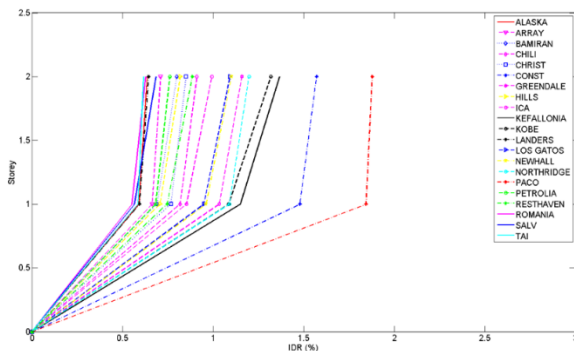


Fig. 5. Peak IDR for the 2-storey structure

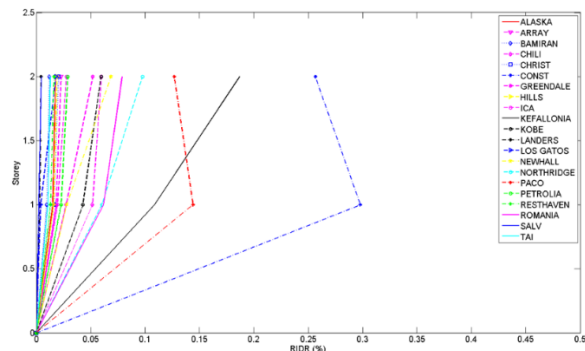


Fig. 6. Peak RIDR for the 2-storey structure

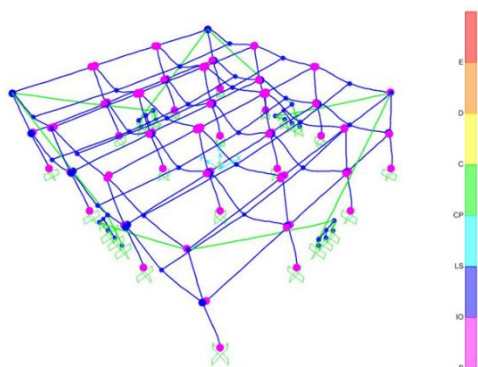


Fig. 7. Worst plastic hinge formation to the 2-storey structure

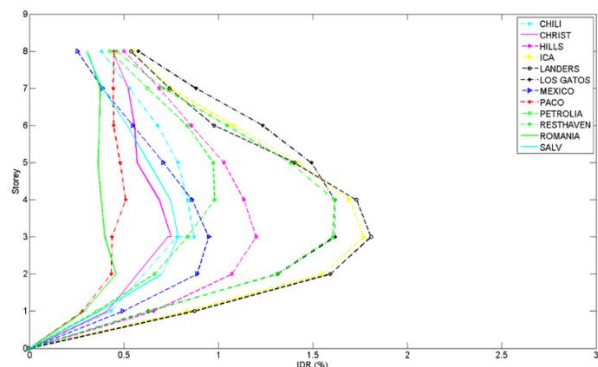


Fig. 8. Peak IDR for the 8-storey structure

Figure 7 shows the worst case of plastic hinge formation to the 2-storey steel structure revealing minor or some damage to frame elements.

The 8-storey steel structure of Fig. 3 exhibits nonlinear behaviour to all seismic ground motions of Table 3. A redesign of the steel structure (not presented herein) should be performed for 12 out of 24 of these motions. In particular, the maximum tensile strength of the spiral strand ropes is exceeded for 5 out of the 24 motions, whereas no damper failure occurred. In 7 out these 24 motions, the maximum RIDR value surpasses the threshold value of 0.5%. Therefore, height wise peak IDR and RIDR distributions for the rest 12 seismic ground motions are shown in Figs.8-9. Figure 10 shows the worst case of plastic hinge formation to the 8-storey steel structure revealing minor or some damage to frame elements.

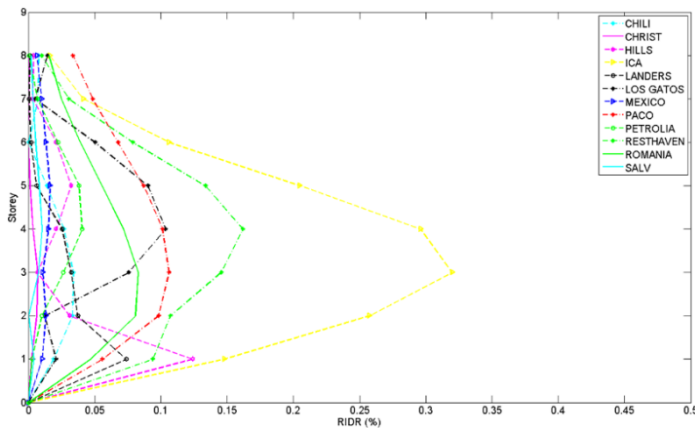


Fig. 9. Peak RIDR for the 8-storey structure

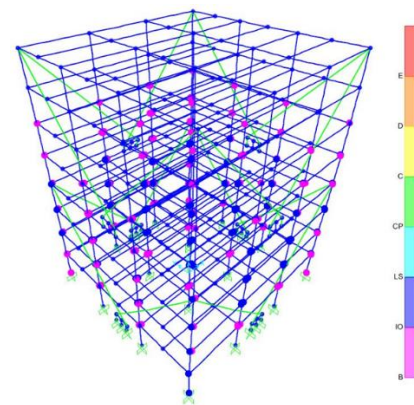


Fig. 10. Worst plastic hinge formation to the 8-storey structure

### 3.2 Steel structures considering SSI

The 2-storey steel structure of Fig. 2 exhibits nonlinear behaviour to 23 out of the 24 seismic ground motions of Table 3. A redesign of the steel structure (not presented herein) should be performed for 3 out of 24 of these motions because the maximum RIDR value surpasses the threshold value of 0.5%. Height wise peak IDR and RIDR distributions for the 2-storey steel structure are shown in Figs.11-12. Figure 13 shows the worst case of plastic hinge formation to the 2-storey steel structure revealing minor or some damage to frame elements.

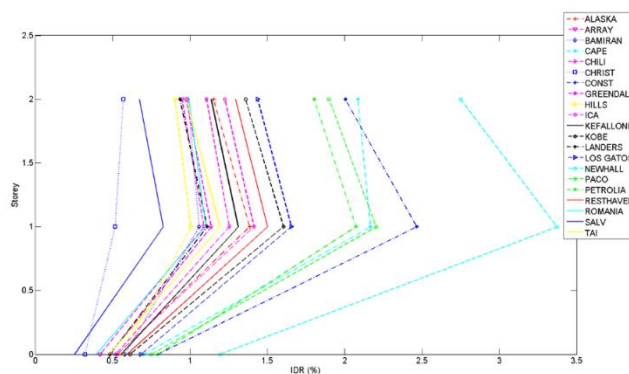


Fig. 11. Peak IDR for the 2-storey structure considering SSI

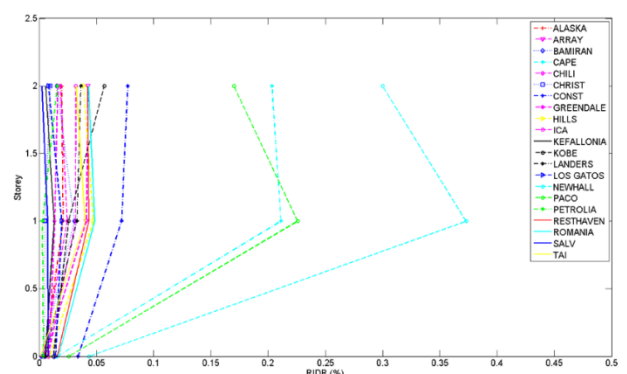


Fig. 12. Peak RIDR for the 2-storey structure considering SSI

The 8-storey steel structure of Fig. 3 exhibits nonlinear behaviour to 22 out of the 24 seismic ground motions of Table 3. A redesign of the steel structure (not presented herein) should be performed for 11 out of 24 of these motions. In particular, the maximum tensile strength of the spiral strand ropes is exceeded for 1 out of the 24 motions, whereas no damper failure occurred. In 10 out these 24 motions, the maximum RIDR value surpasses the threshold value of 0.5%. Therefore, height wise peak IDR and RIDR distributions for the rest 11 seismic ground motions are

shown in Figs.14-15. Figure 16 shows the worst case of plastic hinge formation to the 8-storey steel structure revealing minor or some damage to frame elements.

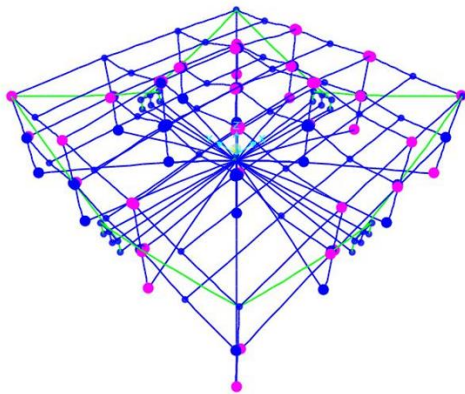


Fig. 13. Worst plastic hinge formation to the 2-storey structure considering SSI

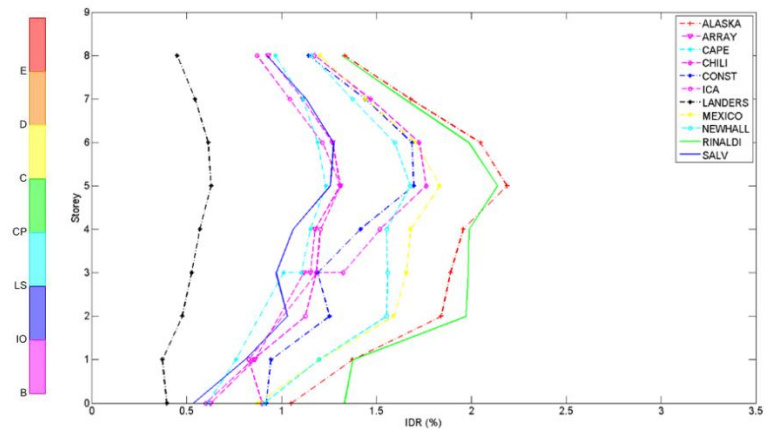


Fig. 14. Peak IDR for the 8-storey structure considering SSI

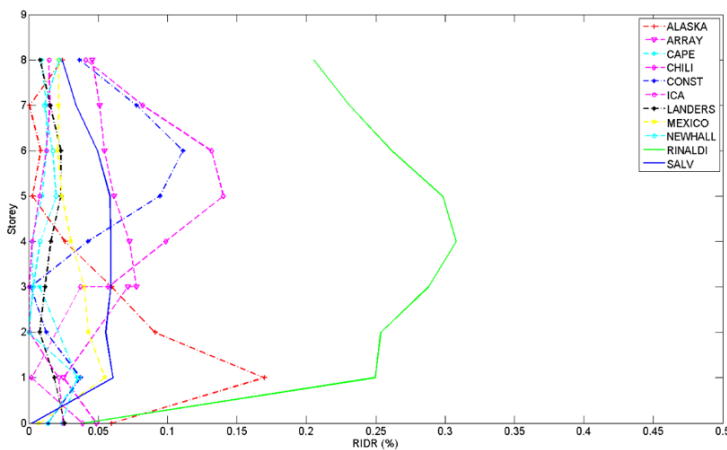


Fig. 15. Peak RIDR for the 8-storey structure considering SSI

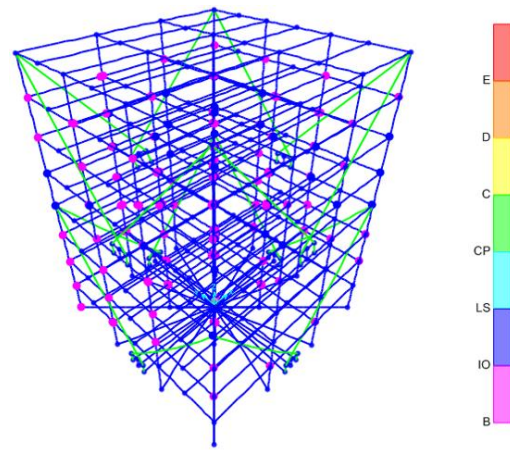


Fig. 10. Worst plastic hinge formation to the 8-storey structure considering SSI

## REFERENCES

1. Katsimpini, Panagiota S., Papagiannopoulos, George A. and Sfakianakis, Manolis G. On the seismic response and damping capacity of low-rise plane steel frames with sessaw system. *Soil Dynamics and Earthquake Engineering*. 2018, 107, pp. 407-416.
2. EC3, Eurocode 3 - Design of steel structures, Part 1-1: General rules and rules for buildings, European Committee for Standardization (CEN), Brussels, 2009.
3. EC3, Eurocode 3 - Design of steel structures, Part 1-8: General rules, seismic actions and rules for buildings, European Committee for Standardization (CEN), Brussels, 2009.
4. EC3, Eurocode 3 - Design of structures with tension components, Part 1-11: General rules, seismic actions and rules for buildings, European Committee for Standardization (CEN), Brussels, 2009.
5. SAP 2000, Static and dynamic finite element analysis of structures [Version 19.0], Computers and Structures, Berkeley, California, 2016.
6. Mulliken, Jeffrey S. and Karabalis, Dimitris L. Discrete model for dynamic through-the-soil coupling of 3-d foundations and structures. *Earthquake Engineering and Structural Dynamics*. 1998, 27, pp. 687-710.
7. EC8, Eurocode 8 - Design of structures for earthquake resistance, Part 5: Foundations, retaining structures and geotechnical aspects, European Committee for Standardization (CEN), Brussels, 2004.